Clim Dyn (2010) 35:285–297
DOI 10.1007/s00382-010-0748-8

Toward the snowball earth deglaciation…

Guillaume Le Hir · Yannick Donnadieu · Gerhard Krinner · Gilles Ramstein

Received: 24 November 2008 / Accepted: 9 January 2010 / Published online: 21 January 2010

Abstract The current state of knowledge suggests that the Neoproterozoic snowball Earth is far from deglaciation even at 0.2 bars of CO_2. Since understanding the termination of the fully ice-covered state is essential to sustain, or not, the snowball Earth theory, we used an Atmospheric General Climate Model (AGCM) to explore some key factors which could induce deglaciation. After testing the models' sensitivity to their parameterizations of clouds, CO_2 and snow, we investigated the warming effect caused by a dusty surface, associated with ash release during a mega-volcanic eruption. We found that the snow aging process, its dirtiness and the ash deposition on the snow-free ice are key factors for deglaciation. Our modelling study suggests that, under a CO_2 enriched atmosphere, a dusty snowball Earth could reach the deglaciation threshold.

Keywords Snowball earth · Albedo · Snow · Deglaciation · Modelling

1 Introduction

The possibility that the Earth suffered episodes of global glaciation has motivated a large number of modelling studies. The original "snowball Earth" hypothesis formulated by Kirschvink (1992) has been updated by Hoffman et al. (1998) and Hoffman and Schrag (2002) owing to additional geological evidences supporting the idea of an entirely ice-covered Earth. Climate model simulations indicate that such a snowball state for the Earth can be induced by anomalously low atmospheric carbon dioxide concentrations (Donnadieu et al. 2004; Hyde et al. 2000), in addition to the Sun being 6% weaker than it is today. Several processes, employing methane (Schrag et al. 2002), the carbonate factory (Ridgwell et al. 2003), the onset of magmatic provinces and their subsequent weathering, or the impact of continental drift on the weathering feedback (Donnadieu et al. 2004; Godderis et al. 2003), have been suggested to produce such low carbon dioxide concentrations. Hence, most of the modelling studies focused on the onset and the physics of a globally ice-covered Earth (e.g., Goodman 2006; Goodman and Pierrehumbert 2003; Pollard and Kasting 2005, 2004; Warren and Brandt 2006; Warren et al. 2002) and it is only recently that the modellers' community has focused on the deglaciation issue. In particular, Pierrehumbert (2004) stated that a partial CO_2 pressure (pCO_2) of 0.12 bar, previously thought to trigger snowball Earth deglaciation (Caldeira and Kasting 1992), was in fact insufficient. Using the General Circulation Model (GCM) FOAM (for Fast Ocean Atmosphere Model), he showed that deglaciation was unlikely even at a pCO_2 of 0.2 bars because of several atmospheric dynamics processes which were not addressed in previous studies mostly based on Energy Balance Models (Pierrehumbert 2005). One of the most striking features was the near-surface inversion of the vertical temperature gradient in winter counteracting the greenhouse effect. As concluding remarks, Pierrehumbert recognized that "some of the highlighted processes impeding the deglaciation with the

G. Le Hir (✉)
Institut de Physique du Globe de Paris, Université Paris, 7-Diderot, 4 place de Jussieu, 75005 Paris, France
e-mail: lehir@ipgp.jussieu.fr

Y. Donnadieu · G. Ramstein
LSCE, CNRS-CEA-UVSQ, 91191 Gif sur Yvette Cedex, France

G. Krinner
LGGE, CNRS and UJF Grenoble, BP 96, 38402 Saint Martin d'Héres Cedex, France

FOAM GCM depended on physical parameterizations being in the most challenging area of the climate dynamics".

Since our main interest is to clarify the conditions required to trigger the deglaciation, our first aim is to test the robustness of this effect using a different GCM: LMDz (Laboratoire de Météorologie Dynamique, Paris, France). In addition to testing the response of the model's parameterizations in an extreme climate, we also evaluate the warming obtained with our model, as a function of the pCO_2, and compare with results from FOAM.

Because of the existence of processes counteracting the greenhouse effect induced by high pCO_2, other potentially warming processes need to be investigated. Amongst them, the dust admixture in the snow, and its deposition on ice, is a good candidate. For that reason, we propose to investigate the snowball Earth climate response when dust particles are emitted into the atmosphere by a volcanic eruption (Mason et al. 2004; Zielinski et al. 1996). Indeed geological records show that catastrophic eruptions have provided aerosols into the atmosphere, but also dust particles which could affect the albedo of a cleaned white surface. As a consequence, a violent eruption may create a dusty Snowball Earth, which may trigger the deglaciation with a lower pCO_2. The largest Quaternary eruption, Toba at 74 ky B.P, released 2×10^{16} g of fine dust (Rampino and Self 1992). Such super-eruptions rarely occur during the Earth history, no more than one or twice per Ma (Mason et al. 2004). Considering the duration of Snowball Earth ($\sim$12 Ma) (Bodiselitsch et al. 2005) and this recurrence rate, an event like Toba likely affected the global glaciation when a large amount of CO_2 had already accumulated in the atmosphere. The effect of smaller eruptions occurring more frequently is also evaluated here.

2 Model and experimental setup

2.1 General setup

The LMD AGCM (Hourdin et al. 2006) is used extensively to investigate present, future and past climates. Model data comparisons for different geological periods show that this tool is able to successfully simulate the last glacial/interglacial cycle (Khodri et al. 2001) as well as earlier climates (Donnadieu et al. 2003; Donnadieu et al. 2002; Ramstein et al. 1997).

For the applications presented here, the spatial resolution is 4° in latitude, 5° in longitude with 19 vertical levels. Our LMDz version uses the Emanuel and Zivkovic-Rothman (1999) moist convection scheme. The cloud and convective parameterizations are coupled following the approach proposed by Bony and Emanuel (2001). Cloud microphysical properties are computed as described in Bony and Emanuel (2001). The cloud optical thickness is computed by using an effective radius of cloud particles set to a constant value for liquid water clouds, and decreasing with decreasing temperature (from 60 to 3.5 μm) for ice clouds (Heymsfield and Platt 1984; Suzuki et al. 1993). Concerning the albedo computation, the ice albedo has a value of 0.65 in the visible spectrum and 0.45 in the near infrared, values consistent with the mean albedo for bare ice measurements (Warren et al. 2002). Our model simulates varying snow depth and fractional cover on the ground, soil albedos being affected by the snow layer. The snow albedo is calculated as a function of aging processes (Rind et al. 1989), and the admixed dust (Krinner et al. 2006). More details about the LMD GCM numerical techniques and physical parameterization are available in Hourdin et al. (2006).

To represent Neoproterozoic conditions, our boundary conditions include a solar constant 6% lower than today (1286 W/m^2), a paleogeography adapted from Torsvik et al. (2001) in which the Rodinia supercontinent occupies an equatorial location and present-day values for orbital parameters. To simulate a Snowball Earth, we prescribed an ocean entirely covered by sea ice, 90% of the continental surface covered by land ice and 10% being left as bare soil.

To reach the equilibrium with Neoproterozoic snowball Earth conditions, our first simulation was performed with 100 ppm of CO_2 imposed during 20 years; the equilibrium was obtained after 10 years. Then, a suite of simulations, lasting 20 years each, was carried out with CO_2 concentration set to 0.0128, 0.1 and 0.2 bar to represent the slow CO_2 accumulation in the atmosphere according to the snowball Earth theory (Hoffman et al. 1998) (SBE simulations). Results were averaged on a sufficient period to obtain a mean climate (the last 5 years for each run). This set of simulations will be compared with FOAM results to evaluate the efficiency of the greenhouse effect as a function of the pCO_2 rise and to test the response of the GCM parameterizations in an extreme climate. Here, we assume that the atmospheric pCO_2 has not exceeded 0.2 bar, notably because GCM radiative codes cannot safely compute the radiative forcing provided by the CO_2 above this value but also for a duration constraint. Indeed, a recent modelling study has demonstrated that accounting for the low-temperature alteration of the oceanic crust, duration for accumulating 0.2 bar of CO_2 is doubled (closer to 20 Ma than 10 Ma) (Le Hir et al. 2008). In addition, recent works (Kendall and Creaser 2006) suggest that the glacial period does not exceed 8 Ma implying a moderate maximum pCO_2 atmospheric level.

2.2 Cloud simulations

Because the Snowball Earth climate is very different from the present day one, the net forcing of clouds could be considerably altered in a very cold climate where the water vapor is strongly reduced (Pierrehumbert 2005). Enhanced cloud forcing requires changes to one of the following parameters: (1) the cloud water content, (2) the cloud particle size, or/and (3) the cloud cover itself and its aspect. Because of the very cold air temperatures, there is no obvious reason to invoke a higher cloud water content, hence the relationship fixing the cloud water content is remained unchanged. To explore the potential global warming or cooling induced by cloud cover changes, a series of sensitivity experiments were conducted by replacing one element or parameter of the reference version, The simulations are performed with 0.2 bar of pCO_2 over 20 years, the last 5 years being used for analysis. The following simulations are considered here:

Cld1 Cld2, Cld3: Since a low water vapor content prevents ice-crystal growth (Walden et al. 2003), the ice-crystal size in ice clouds may have been smaller than observed at present, and thus affected the cloud albedo. To explore this possibility, we ran simulations with a reduced ice-crystal size, the reducing factor being 1.5, 2, and 4, for compared to the reference case (Iacobellis and Somerville 2000). Respectively, we shall refer to this set of simulations as the "Cld1, Cld2, and Cld3" experiments.

Cld4: The second test concerns the potential alteration of the cloud cover and its aspect. Because of the lack of warm oceans and the weak solar heating due to high albedo, deep convection tends to weaken (Pierrehumbert 2005). The quasi-absence of convective clouds might induce a cloud cover dominated by large-scale stratiform clouds. An idealised simulation (Cld4 experiment) has been performed with a modified parameterization of subgrid water (vapor and liquid) distribution such as to increase the cloud cover fraction for a given average humidity (in detail, the variance/mean ratio governing the log-normal clouds distribution (Bony and Emanuel 2001; Hourdin et al. 2006) has been risen by a factor of 10).

2.3 Dust simulations

In a second part, we explore the climate response of a massive dust release into the atmosphere due to a catastrophic volcanic eruption. Using an equilibrated run performed with 0.2 bar of CO_2, we add 2×10^{16} g of fine ash (<2 μm) into the atmosphere. In the Dust1 experiment, we assume that the dust removal by precipitation occurs within ten years, which corresponds to a homogeneous deposition rate of 4 g/m^2 per year. In the Dust2 experiment, we test more rapid fallout (one year), corresponding to a deposition rate of 40 g/m^2 per year. In the Dust3 experiment, we test the impact of a weaker volcanic eruption with a total fallout of 2×10^{15} g evenly distributed over ten years, corresponding to a fallout rate of 0.4 g/m^2 per year.

For calculating the dust content in the snow layer, snow is represented by a two-layer model, with an upper layer of maximum thickness of 8 mm and a lower layer containing the remaining snow mass (Krinner et al. 2006). The surface layer accumulates dust from atmospheric fallout—by dry deposition assumed constant in annual mean. During the melt or sublimation, the snow mass is lost in the upper layer. The dirty snow albedo effect is mainly governed by its depth in the surface. If the snow thickness reaches less than 1 mm, the dust concentration remains unchanged from its preceding time step to prevent a numeric divergence. In consequence the dirty snow alters the surface albedo only if the snowfalls sufficiently overcome the sublimation. If not, the albedo of the surface is set to the albedo of the underlying layer. During snow melting, dust particles remain in place. The snow albedo is estimated using the Marshall and Oglesby formulation (Marshall and Oglesby 1994). An exhaustive description of the deposition module of dust added in LMDz can be found in Krinner et al. (2006).

To compute the snow-free ice albedo as a function of the dust deposition rate, we considered that each volcanic particle was (1) spherical with a diameter reaching 1 μm, (2) characterized by a ρ (mass volume) fixed at 2.7 g/cm^3 (an average value for basaltic rocks), and that each ash layer reaching 10 μm of thickness (or 14 μm accounting for the porosity) hides the underlying surface (Warren, pers com). Finally, the model uses the dust density to compute a surface occupied by an ash layer able to hide the ice surface, which optimize the dust cover spreading. Then the dusty ice albedo is a linear function of the fraction of the surface capped/uncapped by the ash layer (ash albedo: visible, 0.18; near infra-red, 0.35) following Warren (1982) (Fig. 1). To compute the mass of dust available, the model considers the ash directly deposited on the bare ice and dust remaining after the complete melting of the snow cover.

Since our model does not take into account the atmospheric transport of dust, we assume a homogenous deposition of dust, a reasonable assumption considering the extraordinarily widespread Toba ash layer (Ninkovich et al. 1978; Rampino and Self 1988). This worldwide dispersion requires a long residence time in the atmosphere, a phenomenon only possible with very small particles (Fiacco et al. 1994), here typically less than 2 μm. Since such dark particles are sufficiently small to well conduct the absorbed solar energy, they are not heated (Rhodes et al. 1987) and remain on frozen surfaces.

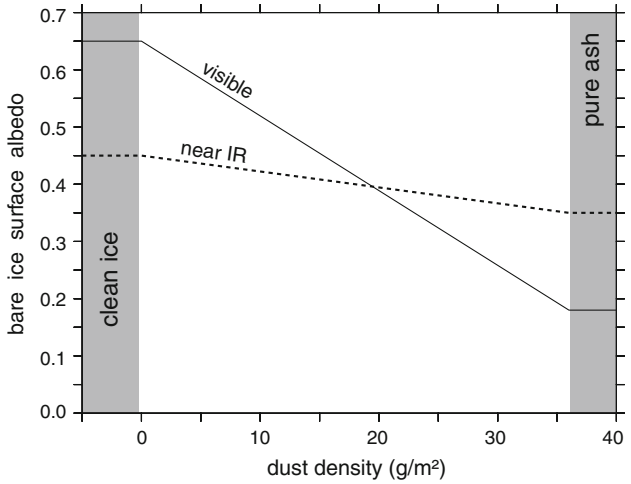

Fig. 1 Bare ice albedo perturbed by the ash deposition. To compute the bare ice albedo as a function of the dust density we have considered that each ash particle was spheric with a diameter reaching 1 μm, with a ρ fixed at 2.7 g/cm^3. 14 μm of ash spherical particles are assumed to be sufficiently opaque to hide the underlying surface. The surface albedo is a linear function of the percent of the ice surface capped/uncapped by an ash layer of 14 μm of thickness. Above a loading of 36 g/m^2, the ice surface becomes entirely ash covered

3 Results

3.1 The climatic response of GCMs

Main results from the experiments obtained with LMDz are summarized in Table 1, and compared with FOAM results. Regarding the effect of a CO_2 rise from 10^{-4} to 0.2 bar, both models predict similar warming (14.2°C for FOAM and 16.9°C in LMDz), confirming by this fact that the snowball Earth climate tends to weaken the greenhouse warming provided by the CO_2, as shown before by Pierrehumbert (2004).

However, for the LMDz model compared to the FOAM runs, the globally averaged annual mean surface air temperature is strikingly different for the same pCO_2. LMDz simulates, respectively at 10^{-4} and 0.2 bar, a global surface temperature 11 and 13.7°C warmer than the FOAM model. In order to explain this difference, a detailed description of the terms contributing to the surface budget is required. The globally averaged surface energy budget can be written as:

$$S_{\text{abs}} = \text{IR} + F_{\text{lat}} + F_{\text{sens}} \quad (1)$$

where F_{lat} is the latent heat, F_{sens} the sensible heat, IR the surface infra-red cooling and S_{abs} the total incoming solar radiation absorbed by the surface. The S_{abs} and IR terms could be defined as following:

$$S_{\text{abs}} = (S/4)A \quad (2)$$

$$\text{IR} = \sigma T s^4 (1 - \varepsilon) \quad (3)$$

A represents the planetary albedo, S the solar constant, ε the CO_2 greenhouse efficiency (i.e. the percent of the IR captured by greenhouse gases), σ and T_s are respectively the Stefan-Boltzmann constant and the surface temperature. Hence, the ΔT depends on several climatic factors: ε, S, A, and surface fluxes F_{latent} and $\Delta F_{\text{sensible}}$.

(1) We consider that ε term is mainly due to CO_2 (Town et al. 2005), a reasonable assumption for the snowball Earth scenario (Hoffman et al. 1998). Figure 2 shows the reduction of outgoing longwave radiation at the tropopause (i.e. the IR energy absorbed by greenhouse gases) calculated with both GCMs' internal radiative module (see Appendix for methodology). The similar evolution of the net long-wave fluxes as a function of the CO_2 for both

Table 1 Comparison of LMDz and FOAM simulations at 10^{-4} and 0.2 bar of CO_2

Climatic factors	pCO_2 10^{-4} bar		pCO_2 0.2 bar		
	FOAM	*LMDz*	*FOAM*	LMDz	LMDz WO–SnAg
Solar constant (S) (W/m^2)	1,278	1,286	1,278	1,286	1,286
Planetary Albedo (CS)	0.64	0.60	0.65	0.60	0.72
Cloud forcing (W/m^2)					
Total	−0.3	5.4	2.1	6.5	−0.3
Short-wave	−1.6	−3.7	−3.0	−7.1	−1.4
Long-wave	1.3	9.1	5.1	13.6	1.1
Latent flux (W/m^2)	4.0	2.8	13.9	10.2	0.65
Sensible flux (W/m^2)	35.6	20.9	34.2	20.2	14.8
Surface temperature (°K)	214.9	225.9	229.1	242.8	207.7
TOA (W/m^2)	−2.04	−2.85	−0.28	−0.31	−3.65

(CS) for Clear Sky diagnostic. WO-SnAg represents the simulation performed without the snow aging process. The TOA budget is defined, at the top of the atmosphere, as the difference between the incoming solar energy minus the energy lost by the outgoing long wave radiations

GCMs reveals that internal computation of CO_2 forcing cannot explain the warmer climate in LMDz. In addition similar patterns for surface thermal inversions in the winter hemisphere (until to 45°N in December) also support a weak warming linked to CO_2. Hence the CO_2 forcing does not cause the difference observed between the two GCMs.

An important remark concerns the near infra-red absorption ($0.7 < \lambda < 5$ μm) by the CO_2. Usually the atmosphere is assumed to be transparent to short waves ($0.2 < \lambda < 5$ μm). However GCMs diverge in strongly CO_2-enriched atmospheres. While FOAM simulates a near infra-red absorption unaffected by CO_2, the LMDz absorption increases with pCO_2. Because this phenomenon affects the atmospheric lapse-rate, LMDz suggests that the deglaciation could occur with a pCO_2 close to 0.1 bar (Le Hir et al. 2007). Both parameterizations being established on available data, it is not possible to state that one parameterization is better than the other (Bonnel and Fouquart 1980; Briegleb 1992). Here, to correctly compare both GCMs, we have adjusted the LMDz solar absorption to match with the FOAM parameterization.

(2) Both GCMs use a solar constant reduced by 6% according to the stellar evolution predicted by Gough (1981), however FOAM runs were performed with an initial solar constant reaching 1,360 W/m^2 where LMDz uses 1,368 W/m^2. This variation represents only 0.5%, which is consistent with the intrinsic evolution of Sun (Damon and Jirikowic 1992), but this initial assumption implies a divergence of 2 W/m^2 in the radiative budget between both GCMs.

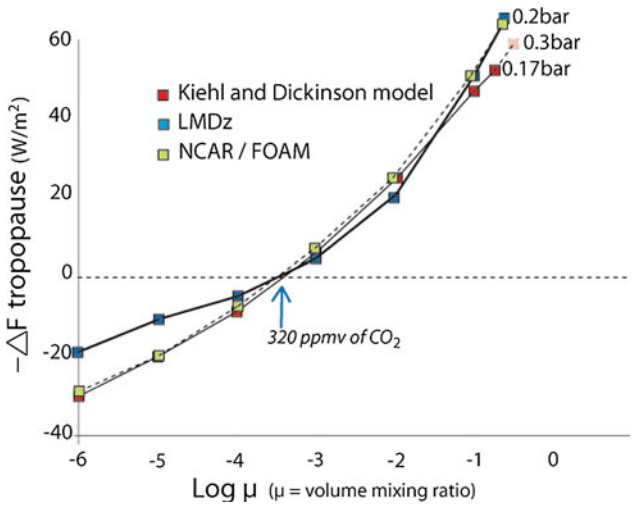

Fig. 2 Net long-wave flux at the tropopause as function of pCO_2. Comparison of net long-wave fluxes computed with the FOAM radiative code, the LMDz radiative module, and the Kiehl-Dickinson radiative model. Close agreement in the radiative forcing between models suggests that LMDz can correctly estimate the warming due to the CO_2 rise until 0.2 bar

(3) A part of the ΔT between both GCMs comes from the surface fluxes, notably the sensible heat flux (Table 1). The energy lost by conduction is very insensitive to the surface temperature, but highly dependent on the surface scheme used in GCMs (Hourdin et al. 2006 and citations therein; Hack et al. 1993 and citations therein). Here, we see that the model parameterization explains a significant part of the ΔT.

(4) The treatment of the surface albedo also strongly differs between the two GCMs. As shown in Table 1, LMDz predicts a planetary albedo lower than FOAM. Since the planetary albedo governs the solar flux received by the Earth system, a greater portion of the net solar influx is absorbed in LMDz than in FOAM model. The snow albedo used in LMDz explains this lower albedo. Although in present day conditions the snow albedo treatment slightly affects the surface energy budget, its parameterization becomes fundamental when the snow-cover tends to be very extended as in snowball Earth. In the LMDz model, the snow albedo is calculated as function of aging process (Chalita and Letreut 1994), according to the formula of Rind et al. (1989). In FOAM this treatment is absent due to a simplification of the CCM2 soil scheme (Hack et al. 1993). Therefore the metamorphosis that leads to a larger snow grain size with time that decreases albedo is not directly taken into account. To balance this parameterization FOAM uses a snow albedo lower than LMDz for fresh snow. LMDz snow albedo varies from 0.95 to 0.9 in the visible spectrum and from 0.7 to 0.4 in the near infra-red as a function of the zenith, and the snow grain size (Marshall and Oglesby 1994). The snow albedo assumed in FOAM reaches 0.8 in visible and 0.45 in infra-red, except on land where the snow albedo is fixed to 0.9 in visible and 0.7 in the near infra-red.

To test the direct impact of the snow aging on the snowball Earth albedo, we have suppressed the snow aging process in a LMDz simulation performed at 0.2 bar pCO_2 (Table 1). Without the snow aging, the fresh snow provides a large planetary albedo increase (0.72 instead of 0.60 in global annual mean) that strongly reduces the mean surface temperature (207.7 K instead of 242.8 K). Differences between the LMDz albedo obtained without snow aging and FOAM run (Table 1) can be explained by the initial higher snow albedo used in LMDz than FOAM, as described previously. This is another example of how GCM parameterizations can affect the Earth temperature in Snowball Earth, and therefore its deglaciation threshold as earlier suggested by Pierrehumbert (2005).

Hence, the albedo parameterization, as well as values for sensitive heat flux and solar constant, explains the warmer climate in LMDz. However to confirm this conclusion, another climatic forcing must be studied: the cloud forcing.

(5) A detailed description of the cloud radiative budget reveals that, for similar air and surface temperatures,

LMDz predicts a cloud heating overcoming the one predicted by FOAM (see Table 1, 10^{-4} bar experiment for LMDz and 0.2 bar experiment for FOAM). This behavior is due to radiative properties of clouds which include a scattering effect (albedo) largely balanced by the infrared trapping (greenhouse effect). In LMDz the longwave forcing is twice as strong as the one obtained in FOAM, the short wave cooling (albedo effect) being very close in both runs. In GCMs, the cloud forcing is controlled by (1) the water condensed in clouds (or cloud water content), (2) the cloud particle size, and (3) by the cloud cover and its distribution. Here, the total cloud cover is quite similar, respectively 86% in LMDz with 10^{-4} bar of CO_2 and 87% in FOAM for 0.2 bar, and the cloud cover distribution is only slightly different (FOAM run predicts more abundant high altitude clouds). Moreover, since the cloud particle size primarily affects the albedo, the strong longwave forcing observed in LMDz is due to a different treatment of the cloud water content. It should be noted that as few observations can be used as guidance to correct the cloud behavior, appropriately representing the effect of clouds in climate models remains a challenge yet. Hence, it is not possible to state that one parameterization is better than the other (Hourdin et al. 2006; Pierrehumbert 2005).

Consequently, two GCMs simulating a hard snowball Earth predict a similar warming by the CO_2 rise but a very different climate in an enriched CO_2 atmosphere (see Table 1). Indeed regarding our study the snowball Earth energy budget can be deeply altered by the surface albedo treatment (Lewis et al. 2006). Clouds play a non-negligible but less critical role than the snow albedo. This is explained by the fact that the snowball Earth is a system covered by snow and clouds. Hence, the CO_2 greenhouse forcing required for deglaciating the Neoproterozoic Snowball Earth is highly model dependent. It should be noted that using LMDz, which has a more favourable parameterization to deglaciate, the annual mean equatorial temperatures reaches 262°K with 0.2 bar of CO_2, which remains far below the melting threshold (Fig. 3), even if some points in tropics can temporarily reach 0°C due to the diurnal influence. This observation is also valid for January (austral summer), moment of the perihelia. Consequently, to explain the termination of Neoproterozoic extremes glaciations, additional factors may have likely contributed to decrease the deglaciation CO_2 threshold. Some potential helping processes, such as cloud properties and snow albedo, are studied hereafter.

3.2 The clouds in the deglaciation problem

Clouds, particularly ice clouds, are notoriously difficult to model. Under present climatic conditions, clouds provide a large cooling effect of about -20 W/m^2 (Kiehl and Trenberth 1997). By contrast, during a snowball Earth event, clouds slightly warm the surface (Table 1), a tendency in agreement with Antarctic measures based on the ERBE database (Pierrehumbert 2005).

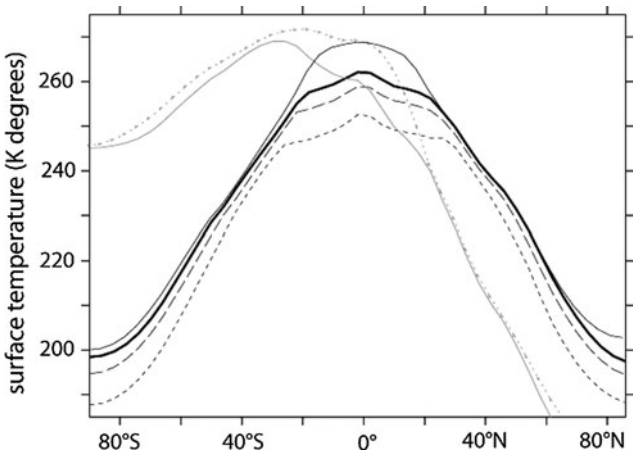

Fig. 3 Zonal surface temperature. *Black curves* represent surface temperature in annual mean averaged in longitude. The *thick black line* is the SBE simulation performed at 0.2 bar. *Dash curves* below the *thick line* represent SBE experiments with a lower pCO_2, respectively 0.1 and 0.0128 bar. The *continuous line*, above the *thick black line*, is the profile temperature obtained with the Dust1 experiment (0.2 bar of CO_2). *Grey curves* represent the January surface temperature predicted with 0.2 bar of CO_2 obtained respectively for SBE run (*thick line*) and Dust1 run (*dash line*). 273 K is the mean annual temperature required to trigger the sea–ice melting (Pierrehumbert 2005)

The difference between the cloud radiative forcing simulated by LMDZ for a pCO_2 of 10^{-4} and 0.2 bar is only 1.1 W/m^{-2}. This means that clouds only provide a weak positive feedback to a warming induced by a CO_2 increase. We conclude that, in standard conditions, clouds play a marginal role in the deglaciation problem. Under snowball Earth conditions, the simulated cold atmospheric temperatures cause the models to predict formation of low, thin ice-clouds characterized by weak emissivity (i.e. greenhouse effect).

Consequently a thin cloud cover seems to be a fairly robust feature of the snowball Earth climate. However, although the clouds' infrared emissivity is probably limited, the low water content of the atmosphere may also affect ice-crystal growth and thus the cloud microphysics. In Cld1, Cld2 and Cld3 experiments the net radiative cloud forcing, caused by the ice-crystal size reduction, remains quasi-unchanged compared to standard conditions (Tables 1, 2). In detail, the long-wave (LW) absorption and short-wave (SW) scattering effect slightly increase with decreasing ice crystal size. Lowering the crystal size enhances the scattering effect, leading to an increased cloud albedo. But, as the IR trapping also depends on the crystal size, the net forcing remains almost unchanged. In short, ice crystal size variations only have a marginal

impact on the radiative budget under snowball Earth conditions and therefore do not provide a solution to the deglaciation problem.

A final test concerns the potential impact of cloud cover itself. Initially with 0.2 bar of CO_2, LMDz predicts that 88% of the Earth is cloud-covered dominated at 90% by large scale clouds, due to the weakness of deep convection (Pierrehumbert 2005). But with an idealised parameterization increasing the cloud cover fraction (Cld4 experiment) the average cloudiness reaches 92% instead of 88 %. This change in the cloud cover aspect provides a substantial surface temperature increase of about 3 K (Table 2). This warming also provides water through evaporation that is transported towards higher atmospheric levels by the Hadley cell. This mechanism enhances the high level cloud formation and thus amplifies the warming. This idealised nebulosity can facilitate deglaciation, but it is unclear which processes could lead to a modified subgrid humidity distribution.

Summarizing the cloud experiments, it is difficult to enhance the net cloud forcing by reasonable assumptions. Predicted atmospheric conditions are unfavourable to formation of thick clouds with a significant warming effect. Even if the Earth is almost entirely cloud covered (Cld4 run), the surface temperature predicted at the equator, 267 K, is not enough to overcome the triggering threshold. Considering our results, additional forcing is required to significantly reduce the required CO_2 threshold to trigger the deglaciation. In this context, the dirty snowball Earth theory with its reduced albedo is investigated next.

3.3 A dusty snowball earth

In a set of sensitivity runs, we add a homogeneous dust deposition rate, setting it to values in the range 0.4–40 g/m^2 per year (see Sect. 2.3). In the Dust1 run, the simulated surface albedo decreases by 0.08 (Fig. 4). Adding the same quantity of dust in one year (instead of 10 years) does not really modulate this result (see Dust2 in Fig. 4). However, decreasing the quantity of dust by an order of magnitude results in a nearly indiscernible effect on albedo and temperature (See Dust3 in Fig. 4). The changes in surface albedo are not homogenously distributed (Fig. 5). Low to mid-latitudes are drastically affected while almost no changes occur at high latitudes.

This pattern mainly comes from the particular precipitation minus evaporation (P − E) budget characterizing a snowball Earth climate. As shown in Fig. 6a, the equatorial area (10°N–10°S) is a planetary net ablation zone while P − E becomes positive within the 10–20° latitudinal band in both hemispheres. As a consequence, the surface albedo of the equatorial band is drastically reduced when including the dust in our GCM experiments (Fig. 5). In details, most of this zone (10°N and 10°S) is annually snow free, due to the moisture convergence in the upward branch of the Hadley circulation at the solstices (Pierrehumbert 2005). In reason of the low thermal inertia of the surface, the Hadley cell position is governed by the seasonal cycle. Since snowfalls are associated to Hadley cell movements, during several months the equatorial P − E budget is positive; hence the equator is temporarily under a no-perennial snow layer (Fig. 6b). At higher latitudes, P − E is globally positive although there are patchy zones characterized by negative P − E.

It is important to note that with our parameterization, the the albedo reduction caused by dust is larger on sea ice than in snow. This behaviour is explained by the fact that ash particles are included into the snow while they remain on the ice surface. In other words, the dust effect is weaker over areas characterized by continuous snow accumulation than over areas where the snow-layer melting or sublimation during summer months leaves a dust layer directly settled on the sea–ice (Fig. 6b). Hence in low latitudes, the decreasing surface albedo is due to the formation of dusty ice and to the very dirty snow caused by the increasing ash concentration in a rather thin snow layer. Conversely, at high latitudes, the continuous fresh snowfalls (Fig. 6) reduce the dust concentration. Therefore the albedo essentially remains unchanged (Fig. 5).

Table 2 Main results of LMDz simulations for the nebulosity effect (simulations performed with 0.2 bar of CO_2)

Clouds simulations	SBE standard	Cld1 standard	Cld2 standard	Cld3 standard	Cld4 stratiform
Ice-crystal size divided by	1	1.5	2	4	1
Cloud forcing (W/m^2)					
Total	6.5	7.1	7.4	7.7	9.5
Short-wave	−7.1	−8.7	−10.0	13.9	−10.3
Long-wave	13.6	15.7	17.4	21.6	19.8
Surface temperature (°K)	242.8	243.0	243.3	243.9	245.9
TOA (W/m^2)	−0.31	−0.71	−0.85	−1.14	3.50

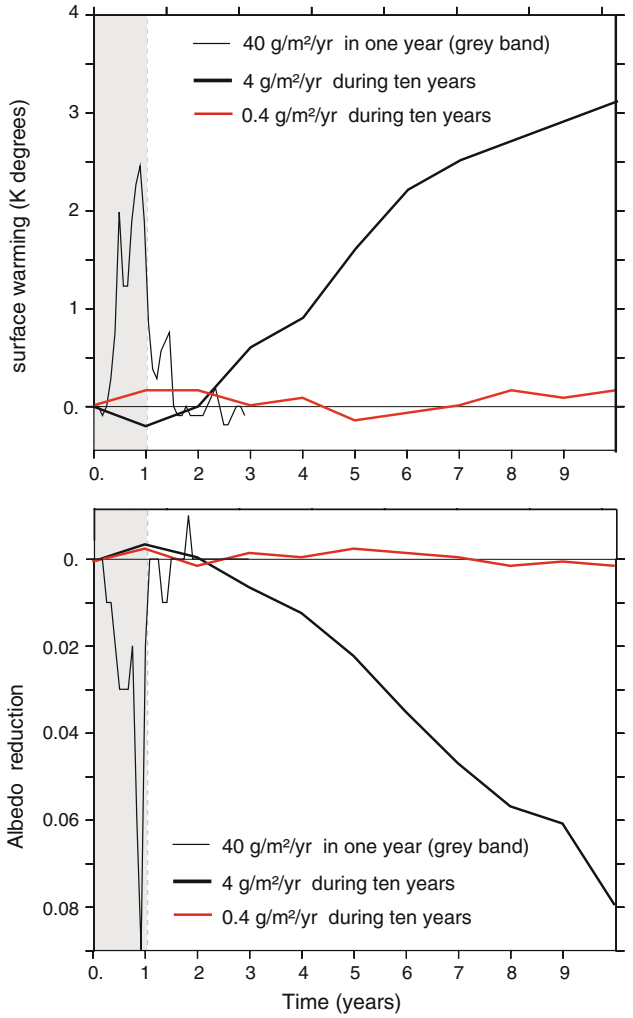

Fig. 4 Surface warming, surface albedo reduction estimations for three scenarios of dust admixture performed at 0.2 bar of CO_2. The *thick black line* represents the dust1 run, the *thinner black line* is the dust2 run, and the *dashed red line* illustrates the dust3 experiment. Dust2 run only: without a model representing the dust transport, the dust covering the sea-ice is artificially removed after the first year

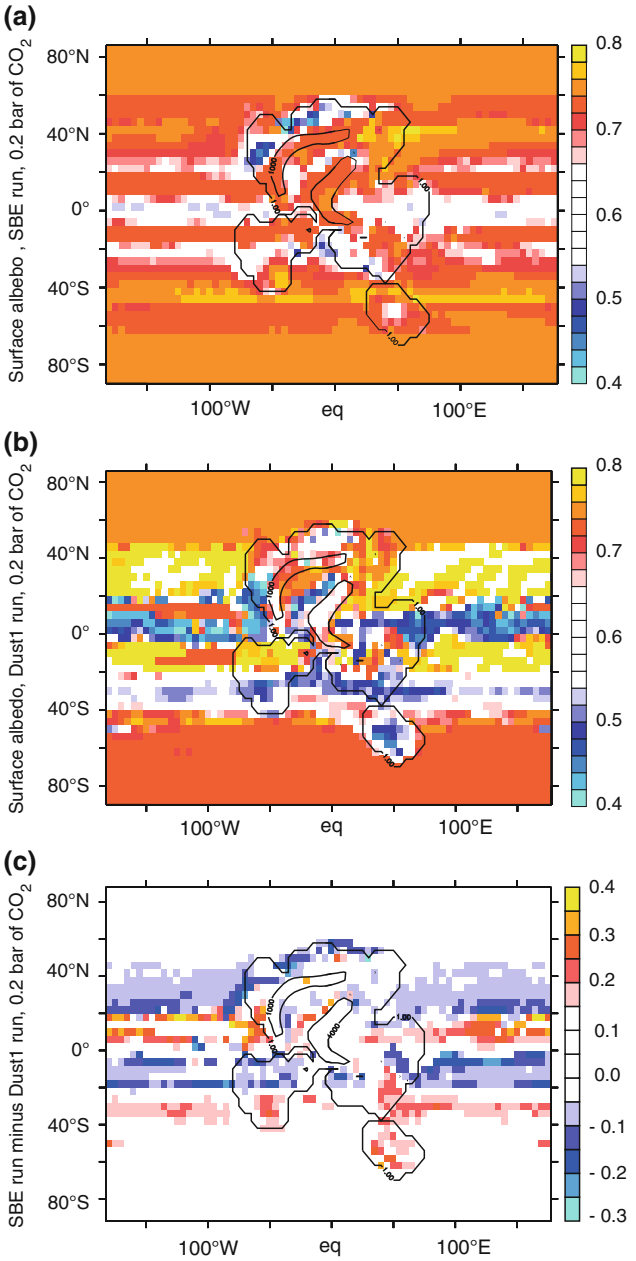

Fig. 5 Surface albedo for (**a**) SBE reference simulation and for (**b**) Dust1 simulation. Dust1 results are plotted for the last year (after 10 years of an imposed ash deposition rate) *Contour lines* represent the continental relief at a fixed level (unit in meter), (**c**) represents SBE run minus Dust1 run, a positive difference represents a reduction of albedo in Dust1 run. High values of albedo between 20 and 40°N obtained in Dut1 run are due to a fresh snow layer. Fresh snowfalls are directly linked to a more active Hadley cell, which explains why this effect is limited to this range of latitudes. The reactivation of the Hadley cell is due to temperatures rise caused by the dust deposition (see Fig. 7)

Looking at the Fig. 7, we see that the annual equatorial temperature, obtained with the Dust1 scenario, is only 2 or 3°C below the deglaciating threshold. Hence an abrupt albedo decrease linked to a massive volcanic eruption seems to be an easy way to trigger the deglaciation. But in the absence of a dust transport model, the movements of the ash cannot be well estimated, notably when ash particles are incorporated into the melted ice. Hence the long term effect of dust cannot be explicitly studied.

4 Discussion

In this paper, one of the issues we address is to what degree the snowball CO_2 melting threshold is model dependent. Using the LMDZ GCM, we confirm the conclusion of a previous study carried out with another model which suggested that, due to processes partially cancelling the near-surface effect of high greenhouse gas concentrations, deglaciating a globally ice-covered Earth requires the

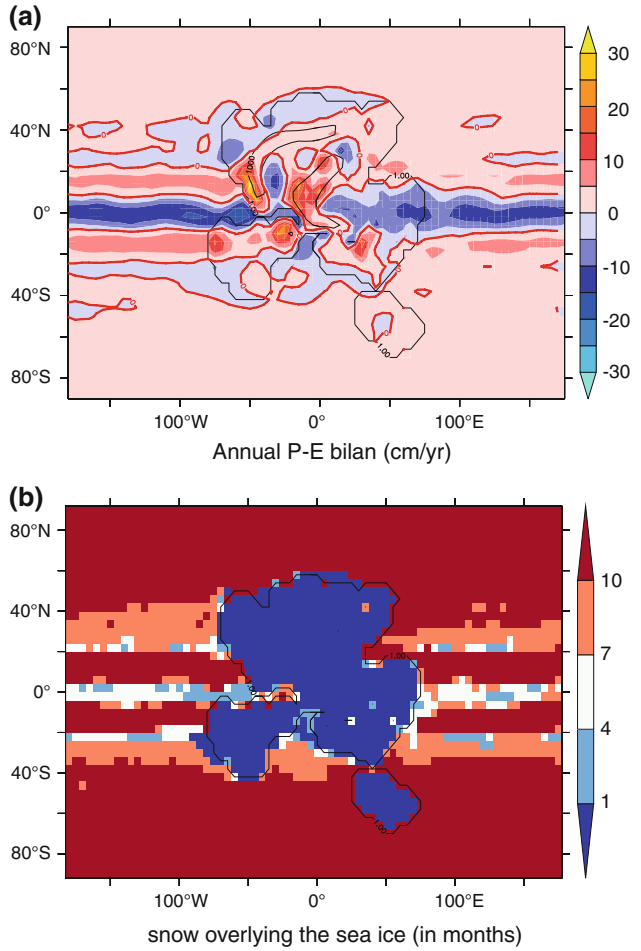

Fig. 6 **a** Annual net balance between precipitations minus evaporation for the SBE reference simulation; (**b**) number of months during which the snow cover overlays the sea–ice (threshold thickness is fixed at 1 mm water equivalent supposing a ρ_{snow} fixed at 330 kg/m^3). The snow covered land ice is masked. *Contour lines* represent the continental relief at a fixed level (unit in meter)

accumulation of a very large amount of CO_2, probably far above 0.2 bar in the absence of other forcings. We also demonstrate that a substantial warming could come from the snow parameterization, notably its aging.

In order to provide the readers with a clear picture of how far away are our runs from the deglaciation, we plot the mean annual surface temperature for the reference run (i.e. SBE run at 0.2 bar), the Cld4 run and the Dust1 run (Fig. 7). The SBE run shows a narrow latitudinal band (5°S–5°N) with a temperature above −12°C. This band expands to 20° latitude in the Cld4 run and remains 4°C below the melting point. The equatorial temperature of the Dust1 run is close to −2°C. In details, as we use an AGCM, the sea–ice is a boundary condition fixed in our set of simulations. Hence the model cannot remove sea ice. Nevertheless, Fig. 7 demonstrates that the dust experiment is close to the melting threshold, in particular because an annual mean temperature close to the melting point implies that the melting point is reached during a significant number of days during the year because of synoptic and seasonal variability, even close to the equator. However finely calculating the real sea–ice melting is not so easy. Indeed if the sea-ice melts at its top, it is formed at its bottom. Hence an oceanic model coupled to a sea ice model taking into account the ice transparency, affected by the dust, would be required to accurately estimate the sea–ice thickness. For that reason, in our study we can only suppose that the sea ice should disappear at the equator.

Nevertheless, several factors have still to be accounted for before putting an end to the snowball deglaciation debate. One of them is the duration required to melt the thick sea–ice. Regarding our volcanic eruptions scenario, our results suggest that dust affects the albedo during ∼10 years. A sea–ice cover of about 100 m thickness at low latitudes was inferred for a hard snowball Earth state (Goodman 2006; Goodman and Pierrehumbert 2003; Warren et al. 2002). At least 10 m of sea–ice should therefore be removed each year to trigger the oceanic feedback loop leading to deglaciation. Considering net ice ablation rates usually assumed to vary between 15 and 35 cm/year (McKay 2000), triggering the deglaciation would require a reduced ice albedo during a much longer period. This time constrain becoming more problematic when we consider the weakness of sublimation rates obtained by GCMs during snowball events (Pollard and Kasting 2004, 2005). Hence, a short eruption would not be able to entirely melt the sea–ice thickness. A second reason limiting the dusty snowball Earth theory comes from processes that are not described in our study, as the solar influx reduction due to the atmospheric opacity rise induced by dust and sulphates emissions into the atmosphere during a volcanic eruption.

If our modelling study shows warmer surface temperatures, a part of the mechanism explaining the melting procedure seems to be lacking. In this context, it would be interesting to examine some other processes being able to extend the warming initiated by the ash released linked to volcanic eruptions. Amongst the solutions (1) a very recent, proposed by Kennedy et al. (2008), could be a large CH_4 release by hydrate destabilisation. In this context, the volcanic eruption could be the cause of the massive methane hydrates destabilisation (Maslin et al. 2004). Since a very cold atmosphere tends to increase the methane lifetime (Le Hir et al. 2007), its effect could operate long enough to melt the thick sea ice (2) A second very interesting solution would be puddle formation occurring when the ice begins to melt (Fetterer and Untersteiner 1998; Perovich et al. 2002) Measurements indicate a puddle albedo of about 0.3. Puddle formation thus dramatically reduces the ice albedo (Perovich et al. 2002; Krinner et al. 2009; Fetterer and

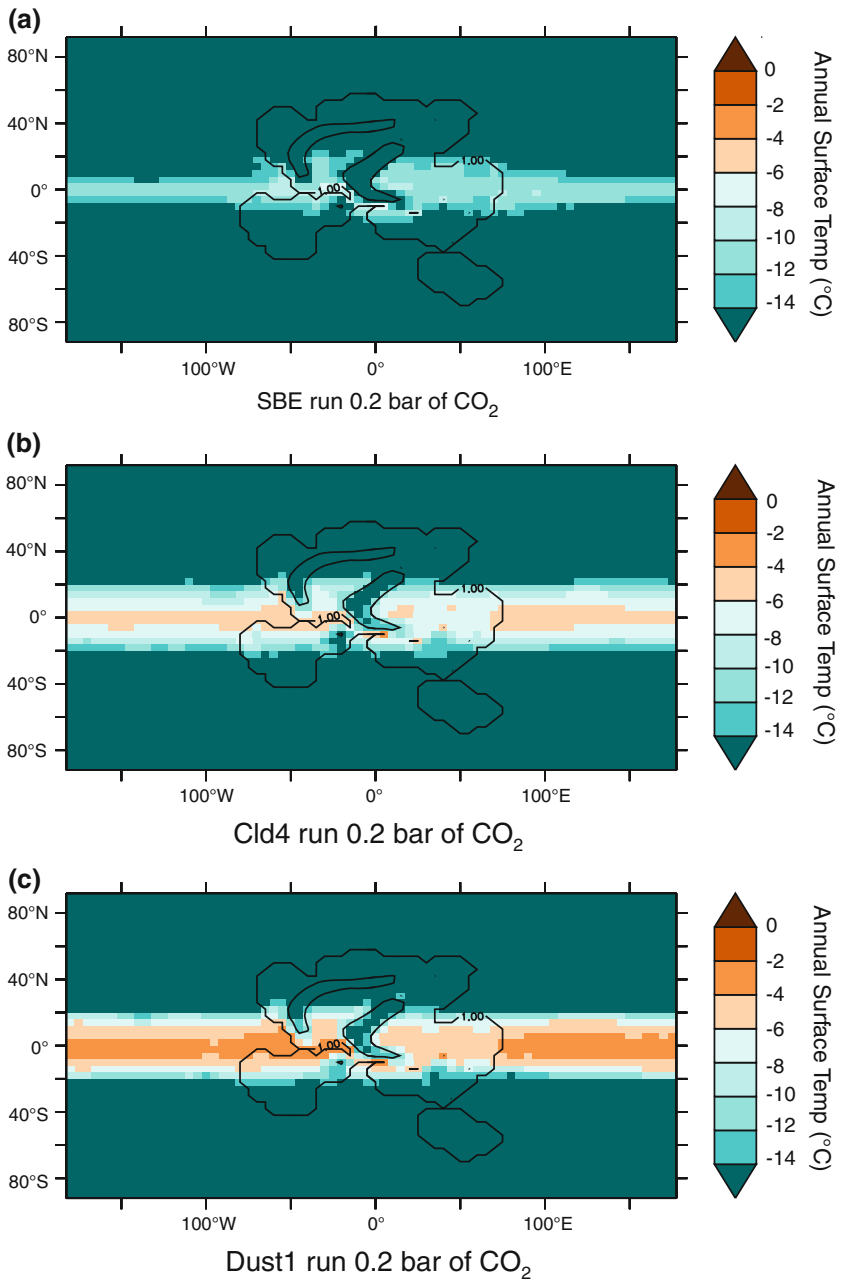

Fig. 7 Mean annual surface temperature (°C) for three runs (**a**) SBE reference run (*upper*), (**b**) Cld4 run (*middle*), (**c**) Dust1 run (*lower*). Dust1 temperature is plotted for the last year (after 10 years of an imposed ash deposition rate). *Contour lines* represent the continental relief at a fixed level (unit in meter)

Untersteiner 1998). Hence, the puddle formation could provide a strong positive heating feedback able to complete the snowball Earth deglaciation.

5 Conclusion

The processes leading to the melting of a snowball Earth were not widely studied up to now, because the mega-greenhouse effect simulated with an EBM suggested that 0.12 bars was enough to end the snowball event. This scenario was dismissed by Pierrehumbert (2004) suggesting that very high CO_2 atmospheric mixing ratio was required to trigger the deglaciation. Here, we show that the CO_2 threshold is model dependent due to the cloud and albedo parameterization and, that fine ash particles released by a massive volcanic eruption is a likely process to explain the abrupt deglaciation. Without causing the entire melting of the thick equatorial sea–ice, we argue that a large eruption, like Toba or bigger, occurring when the atmosphere is already enriched in CO_2, could be the critical factor to shift the Earth system from

a totally glaciated Earth to rapid deglaciation. Finally, up to now, the snowball climate remains a challenge to our understanding of climate. Although some geological records appear to challenge the existence of snowball earth, nothing in the records and models clearly knocks this attractive theory out of the running.

Acknowledgments The authors thank the two reviewers, R. Pierrehumbert for his constructive review and comments on the snowball Earth climate, and S. Warren for his very detailed and interesting review, notably his helpful comments concerning interactions between sea-ice albedo and ash particles deposition. J.L Dufresne is thanked for discussion of an earlier version of the manuscript. This research was supported by INSU, this work being a contribution to the ANR project Accro-Earth. We used computer resources at CCRT/CEA. This is IPGP contribution no. 2587.

Appendix

In LMDz, the radiation scheme is the one introduced several years ago in the model of the European Centre for Medium-Range Weather Forecasts (ECMWF) by Morcrette: the solar part is a refined version of the scheme developed by Bonnel and Fouquart (1980) and the thermal infra-red part is due to Morcrette and Fouquart (1986). The radiative active species are H_2O, O_3, CO_2, O_2, N_2O, CH_4, NO_2 and CFCs.

Working with high pCO_2 requires that we check the validity of our radiative code, in order to correctly simulate the greenhouse warming due to CO_2 rise.

The thermal infra-red part ($\lambda > 5$ µm)

An important parameter in estimating the CO_2 effect is the change in the net radiative flux at the tropopause for a given temperature structure (here the US standard profile). To compare our radiative module, we have calculated the evolution of outgoing longwave radiation, using several CO_2 partial pressures, with the LMDz radiative module, the FOAM radiative module (coming from the CCM3) and the polynomial fit developed by Kiehl and Dickinson (hereafter cited as K-D model) in their radiative-convective model based on the US standard profile (Kiehl and Dickinson 1987). The change in net long-wave flux from LMDz, K-D model, and FOAM radiative module, is shown in Fig. 1. Those expressions have been validated up to 0.17 bar by the authors for the K-D model and up to 0.2 bar for FOAM (Pierrehumbert 2004). The net long-wave flux comparison at high concentrations of atmospheric CO_2 indicates that LMDz radiative module is appropriated for estimating the radiative infra-red effects of large amounts of CO_2.

The solar part ($0.2 < \lambda < 5$ µm)

It should be noted that the radiative module of GCM includes the near infra-red in their short wave computation. This parameterization supposes that the CO_2 rise can affect the radiative budget. An initial comparison between FOAM and LMDz radiative modules revealed a short wave absorption considerably greater in LMDz than FOAM. One of the main consequences of this behavior was that, in LMDz GCM simulations, the atmospheric lapse rate was altered at high pCO_2 due to this significant solar absorption. Since the direct warming of the greenhouse effect depends on the lapse rate, the surface temperature predicted initially with LMDz was potentially overestimated (Le Hir et al. 2007). Both parameterizations being established on available data, it is not possible to state that one parameterization is better than the other (Bonnel and Fouquart 1980; Briegleb 1992). We just remark that both parametrizations used in those GCMs have not been recently updated. For that reason, to correctly compare FOAM and LMDz in this study, we have adapted the solar absorption in the LMDz radiative module to approximate the FOAM results.

References

Bodiselitsch B, Koeberl C, Master S, Reimold WU (2005) Estimating duration and intensity of Neoproterozoic snowball glaciations from Ir anomalies. Science 308:239–242

Bonnel BF, Fouquart Y (1980) Computations of solar heating of the earth's atmosphere: a new parameterization. Contrib Atmos Phys 53:35–62

Bony S, Emanuel KA (2001) A parameterization of the cloudiness associated with cumulus convection: evaluation using TOGA COARE data. J Atmos Sci 58:3158–3183

Briegleb BP (1992) Delta-Eddington approximation for solar-radiation in the NCAR Community Climate Model. J Geophys Res Atmos 97:7603–7612

Caldeira K, Kasting JF (1992) Susceptibility of the early earth to irreversible glaciation caused by carbon dioxide clouds. Nature 359:226–228

Chalita S, Letreut H (1994) The Albedo of Temperate And Boreal Forest and the Northern-Hemisphere Climate—a sensitivity experiment using the Lmd-Gcm. Clim Dyn 10:231–240

Damon PE, Jirikowic JL (1992) The sun as a low-frequency harmonic-oscillator. Radiocarbon 34:199–205

Donnadieu Y, Ramstein G, Fluteau F, Besse J, Meert J (2002) Is high obliquity a plausible cause for Neoproterozoic glaciations? Geophys Res Lett 29. doi:10.1029/2002GL015902

Donnadieu Y, Fluteau F, Ramstein G, Ritz C, Besse J (2003) Is there a conflict between the Neoproterozoic glacial deposits and the snowball Earth interpretation: an improved understanding with numerical modeling. Earth Planet Sci Lett 208:101–112

Donnadieu Y, Godderis Y, Ramstein G, Nedelec A, Meert J (2004) A 'snowball Earth' climate triggered by continental break-up through changes in runoff. Nature 428:303–306

Emanuel KA, Zivkovic-Rothman M (1999) Development and evaluation of a convection scheme for use in climate models. J Atmos Sci 56(11):1766–1782

Fetterer F, Untersteiner N (1998) Observations of melt ponds on Arctic sea ice. J Geophys Res 103(C11):24:821–824. doi: 10.1029/98JC02034

Fiacco RJ, Thoardason T, Germani MS, Self S, Palais JM, Whitlow S, Grootes PM (1994) Atmospheric aerosol loading and transport due to the 1883–1884 Laki eruption in Iceland, interpreted form ash particles and acidity in the GISP2 ice core. Quat Res 42(3):231–240

Godderis Y, Donnadieu Y, Nedelec A, Dupre B, Dessert C, Grard A, Ramstein G, Francois LM (2003) The Sturtian 'snowball' glaciation: fire and ice. Earth Planet Sci Lett 211:1–12

Goodman JC (2006) Through thick and thin: marine and meteoric ice in a "snowball earth" climate. Geophys Res Lett 33:L16701. doi:10.1029/2006GL026840

Goodman JC, Pierrehumbert RT (2003) Glacial flow of floating marine ice in ''snowball earth''. J Geophys Res Oceans 108. doi: 10.1029/2002JC001471

Gough DO (1981) Solar interior structure and luminosity variations. Solar Phys 74:21–34

Hack JJ, Boville BA, Briegleb BP, Kiehl JT, Rasch PJ, Williamson DL (1993). Description of the NCAR Community Climate Model (CCM2). NCAR Technical Note NCAR/TN-382+STR

Heymsfield AJ, Platt CMR (1984) A parameterization of the particle-size spectrum of ice clouds in terms of the ambient-temperature and the ice water-content. J Atmos Sci 41:846–855

Hoffman PF, Schrag DP (2002) The snowball earth hypothesis: testing the limits of global change. Terra Nova 14:129–155

Hoffman PF, Kaufman AJ, Halverson GP, Schrag DP (1998) A Neoproterozoic snowball earth. Science 281:1342–1346

Hourdin F, Musat I, Bony S, Braconnot P, Codron F, Dufresne JL, Fairhead L, Filiberti MA, Friedlingstein P, Grandpeix JY, Krinner G, Levan P, Li ZX, Lott F (2006) The LMDZ4 general circulation model: climate performance and sensitivity to parametrized physics with emphasis on tropical convection. Clim Dyn 27:787–813

Hyde WT, Crowley TJ, Baum SK, Peltier WR (2000) Neoproterozoic 'snowball earth' simulations with a coupled climate/ice-sheet model. Nature 405:425–429

Iacobellis SF, Somerville RCJ (2000) Implications of microphysics for cloud-radiation parameterizations: lessons from TOGA COARE. J Atmos Sci 57:161–183

Kendall B, Creaser RA (2006) Re-Os systematics of the Proterozoic Velkerri and Wollogorang black shales, McArthur basin, Northern Australia. Geochim Cosmochim Acta 70:A314

Kennedy M, Mrofka D, von der Borch C (2008) Snowball earth termination by destabilization of equatorial permafrost methane clathrate. Nature 453:642–645

Khodri M, Leclainche Y, Ramstein G, Braconnot P, Marti O, Cortijo E (2001) Simulating the amplification of orbital forcing by ocean feedbacks in the last glaciation. Nature 410:570–574

Kiehl JT, Dickinson RE (1987) A study of the radiative effects of enhanced atmospheric CO_2 and CH_4 on early earth surface temperature. J Geophys Res 92:2991–2998

Kiehl JT, Trenberth KE (1997) Earth's annual global mean energy budget. Bull Am Meteorol Soc 78:197–208

Kirschvink JL (1992) Late proterozoic low-latitude glaciation: the snowball earth. In: Schopf JW, Klein C (eds) The proterozoic biosphere. Cambridge University Press, Cambridge, pp 51–52

Krinner G, A Rinke et al (2009) Impact of prescribed Arctic sea ice thickness in simulations of the present and future climate. Clim Dyn. doi:10.1007/s00382-009-0587-7

Krinner G, Boucher O, Balkanski Y (2006) Ice-free glacial northern Asia due to dust deposition on snow. Clim Dyn 27:613–625

Le Hir G, Ramstein G, Donnadieu Y, Pierrehumbert RT (2007) Investigating plausible mechanisms to trigger a deglaciation from a hard snowball earth. Comptes Rendus Geosci 339:274–287

Le Hir G, Ramstein G, Donnadieu Y, Godderis Y (2008) Scenario for the evolution of atmospheric *p*CO2 during a snowball earth. Geology 36:47–50

Lewis JP, Weaver AJ, Eby M (2006) Deglaciating the snowball Earth: sensitivity to surface albedo. Geophys Res Lett 33

Marshall S, Oglesby RJ (1994) An improved snow hydrology for gcms.1: snow cover fraction, albedo, grain-size, and age. Clim Dyn 10:21–37

Maslin M, Owen M, Day S, Long D (2004) Linking continental-slope failures and climate change: testing the clathrate gun hypothesis: Geology 32:53–56

Mason BG, Pyle DM, Oppenheimer C (2004) The size and frequency of the largest explosive eruptions on earth. Bull Volcanol 66:735–748

McKay CP (2000) Thickness of tropical ice and photosynthesis on a snowball earth. Geophys Res Lett 27:2153–2156

Morcrette JJSL, Fouquart Y (1986) Pressure and temperature dependence of the absorption in longwave radiation parameterizations. Contrib Atmos Phys 59:455–469

Ninkovich D, Shackleton NJ et al (1978) K–Ar age of late pleistocene eruption of Toba, North Sumatra. Nature 276:574–577

Perovich DK, Grenfell TC, Light B, Hobbs PV (2002) Seasonal evolution of the albedo of multiyear Arctic sea ice. J Geophys Res Oceans 107(C10). doi:10.1029/2000JC000438

Pierrehumbert RT (2004) High levels of atmospheric carbon dioxide necessary for the termination of global glaciation. Nature 429:646–649

Pierrehumbert RT (2005) Climate dynamics of a hard Snowball Earth. J Geophys Res 110. doi:10.1029/2004JD005162

Pollard D, Kasting JF (2004) Climate-ice sheet simulations of neoproterozoic glaciation before and after collapse to snowball earth. The Extreme Proterozoic: Geology, Geochemistry, and Climate. Geophysical Monograph series 146

Pollard D, Kasting J.F (2005) Snowball earth: a thin-ice solution with flowing sea glaciers. J Geophys Res Oceans 110. doi: 10.1029/2004JC002525

Rampino MR, Self S (1992) Volcanic winter and accelerated glaciation following the toba super-eruption. Nature 359:50–52

Rampino MR, Self S et al (1988) Volcanic Winters. Annu Rev Earth Planet Sci 16:73–99

Ramstein G, Fluteau F, Besse J, Joussaume S (1997) Effect of orogeny, plate motion and land sea distribution on Eurasian climate change over the past 30 million years. Nature 386:788–795

Rhodes J, Armstrong RL, Warren SG (1987) Mode of formation of "ablation hollows" controlled by dirt content of snow. J Glaciol 33(114):135–139

Ridgwell AJ, Kennedy MJ, Caldeira K (2003) Carbonate deposition, climate stability, and neoproterozoic ice ages. Science 302:859–862

Rind D, Peteet D, Kukla G (1989) Can Milankovitch orbital variations initiate the growth of ice sheets in a general-circulation model. J Geophys Res Atmos 94:12851–12871

Schrag DP, Berner RA, Hoffman PF, Halverson GP (2002) On the initiation of a snowball Earth. Geochem Geophys Geosyst 3. doi: 10.1029/2001GC000219

Suzuki T, Tanaka M, Nakajima T (1993) The microphysical feedback of cirrus cloud in climate-change. J Meteorol Soc Jpn 71:701–714

Torsvik TH, Carter LM, Ashwal LD, Bhushan SK, Pandit MK, Jamtveit B (2001) Rodinia refined or obscured: palaeomagnetism of the Malani igneous suite (NW India). Precambr Res 108:319–333

Town MS, Walden VP et al (2005) Spectral and broadband longwave downwelling radiative fluxes, cloud radiative forcing, and fractional cloud cover over the South Pole. J Clim 18(20):4235–4252

Walden VP, Warren SG, Tuttle E (2003) Atmospheric ice crystals over the Antarctic Plateau in winter. J Appl Meteorol 42:1391–1405

Warren SG (1982) Optical-properties of snow. Rev Geophys 20(1):67–89

Warren SG, Brandt RE (2006) Comment on "snowball earth: a thin-ice solution with flowing sea glaciers'' In: Pollard D, Kasting JF. J Geophys Res Oceans 111. doi:10.1029/2005JC003411

Warren SG, Brandt RE, Grenfell TC, McKay CP (2002) Snowball earth: ice thickness on the tropical ocean. J Geophys Res Oceans, 107. doi:10.1029/2001JC001123

Zielinski GA, Mayewski PA, Meeker LD, Whitlow S, Twickler MS, Taylor K (1996) Potential atmospheric impact of the Toba mega-eruption similar to 71,000 years ago. Geophys Res Lett 23:837–840